Laukkanen, Olli-Ville; Winter, H. Henning

Strain accumulation in bituminous binders under repeated creep-recovery loading predicted from small-amplitude oscillatory shear (SAOS) experiments

Published in:
Mechanics of Time Dependent Materials

DOI:
10.1007/s11043-017-9373-9

Published: 01/01/2018

Document Version
Peer-reviewed accepted author manuscript, also known as Final accepted manuscript or Post-print

Please cite the original version:
Laukkanen, O.-V., & Winter, H. H. (2018). Strain accumulation in bituminous binders under repeated creep-recovery loading predicted from small-amplitude oscillatory shear (SAOS) experiments. *Mechanics of Time Dependent Materials*. https://doi.org/10.1007/s11043-017-9373-9

Strain accumulation in bituminous binders under repeated creep-recovery loading predicted from small-amplitude oscillatory shear (SAOS) experiments

Olli-Ville Laukkanen[*,1,2], *H. Henning Winter*[1]

[1] *Department of Polymer Science and Engineering and Department of Chemical Engineering, University of Massachusetts, Amherst, Massachusetts 01003, United States*

[2] *Department of Chemical and Metallurgical Engineering, School of Chemical Engineering, Aalto University, PO Box 16100, 00076, Aalto, Finland*

[*] *corresponding author: email: olaukkanen@mail.pse.umass.edu; phone: (+1) 413-230-1541*

Abstract The creep-recovery (CR) test starts out with a period of shearing at constant stress (creep) and is followed by a period of zero shear stress where some of the accumulated shear strain gets reversed. Linear viscoelasticity (LVE) allows to predict the strain response to repeated creep-recovery (RCR) loading from measured small-amplitude oscillatory shear (SAOS) data. Only the relaxation and retardation time spectra of a material need to be known and these can be determined from SAOS data. In an application of the Boltzmann superposition principle (BSP), the strain response to RCR loading can be obtained as linear superposition of the strain response to many single creep-recovery tests. SAOS and RCR data were collected for several unmodified and modified bituminous binders, and the measured and predicted RCR responses were compared. Generally good agreement was found between the measured and predicted strain accumulation under RCR loading. However, in the case of modified binders, the strain accumulation was slightly overestimated (≤20 % relative error) due to the insufficient SAOS information at long relaxation times. Our analysis also demonstrates that the evolution in the strain response under RCR loading, caused by incomplete recovery, can be reasonably well predicted by the presented methodology. It was also shown that the outlined modeling framework can be used, as a first approximation, to estimate the rutting resistance of bituminous binders by predicting the values of the Multiple Stress Creep Recovery (MSCR) test parameters.

Keywords Rheology; Creep-recovery; Bituminous binders; Boltzmann superposition principle; Rutting

Acknowledgement The authors would like to thank Dr. Hilde Soenen (Nynas NV) for providing access to the rheological experimental data used in the present analysis.

1 Introduction

The rheological behavior of viscoelastic materials can be characterized by various test methods such as oscillatory shear, stress relaxation (step strain), shear creep followed by recovery, and rotational viscometry (Ferry 1980; Mezger 2006). Shear creep and creep recovery (hereafter, for brevity, referred to merely as creep-recovery) is among the most practical rheological measurement techniques, being particularly suitable for obtaining viscoelastic properties in the terminal regime, i.e. at low frequencies or long loading times (Münstedt 2014). In addition, creep-recovery tests can serve as a powerful tool to distinguish between recoverable viscoelastic deformation and non-recoverable viscous deformation (Delgadillo et al. 2006). A comprehensive review of the many advantages of creep-recovery tests is given by Münstedt (Münstedt 2014). Despite of the undeniable benefits, creep-recovery tests have only recently become popular, especially in the asphalt community for characterizing the performance of asphalt binders at high service temperatures (Bahia et al. 2001; D'Angelo et al. 2007). In particular, repeated creep-recovery (RCR) tests are routinely used to assess the rutting resistance of bituminous binders (D'Angelo 2009; Laukkanen et al. 2015).

It helps that the creep-recovery response of a material may be obtained from small-amplitude oscillatory shear (SAOS) measurements by using the well-known interrelationships of linear viscoelasticity theory as shown in this paper. In some cases, creep-recovery properties might be even more readily obtained through the calculation from SAOS data than by direct measurement. This is of great practical importance because experience has shown that experimental creep-recovery data are often prone to instrument-related artifacts, such as the residual torque of the bearing, the momentum of inertia of the rotor and the bearing friction (Münstedt 2014; Gabriel and Kaschta 1998), as well as to poor repeatability and reproducibility (Soenen et al. 2013). Although the relationships between SAOS and linear viscoelastic creep-recovery properties are well established, there have not been any studies systematically investigating the possibility to predict strain accumulation under RCR loading from SAOS experiments. In particular, there is no knowledge of possible experimental limitations of this type of data conversion.

In this study, a theoretical framework for predicting strain accumulation under RCR loading is presented. We employ the theory of linear viscoelasticity in such a way that only SAOS data are needed to generate predictions of RCR behavior. To our knowledge, there are no earlier studies in which strain accumulation under RCR loading has been predicted based solely on SAOS data. In this article, theoretical predictions of RCR strain are compared with the experimental RCR data of various unmodified and modified bituminous binders. Experimental limitations influencing the accuracy of these predictions are discussed. The RCR predictions are used to estimate the values of the Multiple Stress Creep Recovery (MSCR) test parameters in an effort to assess the rutting resistance of bituminous binders. However, this study limits itself primarily to the linear viscoelastic (LVE) creep-recovery behavior. A detailed analysis of how to predict nonlinear viscoelastic creep-recovery behavior remains the subject of future studies.

2 The single creep-recovery experiment in the LVE regime

A creep-recovery experiment, Fig. 1, starts out with the application of a shear stress σ_0 at $t = 0$. The stress is kept constant for a predefined duration, the creep time t_c. While this is done, the shear strain $\gamma(t)$ is monitored as a function of time. Typically, the measured shear strain gets normalized with respect to the applied creep stress to obtain the shear creep compliance

$$J(t) = \frac{\gamma(t)}{\sigma_0} \qquad \text{for } 0 < t < t_c \qquad (1)$$

At $t = t_c$, the second part of the experiment begins by setting and keeping the stress at zero thereby allowing the material to retract from the deformation induced by the applied stress. The sample is contained by the shear fixtures of the rheometer during the recovery. Again, the shear strain is monitored as a function of time and a stress-normalized value for material response can be expressed as the recoverable creep compliance

$$J_r(t_r, t_c) = \frac{\gamma_r(t_r,t_c)}{\sigma_0} \qquad \text{for } t_c < t \qquad (2)$$

$\gamma_r(t_r,t_c) = \gamma(t_c) - \gamma(t)$ is the portion of the shear strain that recovers during the recovery time, $t_r = t - t_c$. One should note that the amount of strain recovery, and thus the value of the recoverable creep compliance J_r, depends on the creep time as long as steady-state conditions have not been reached in the creep phase.

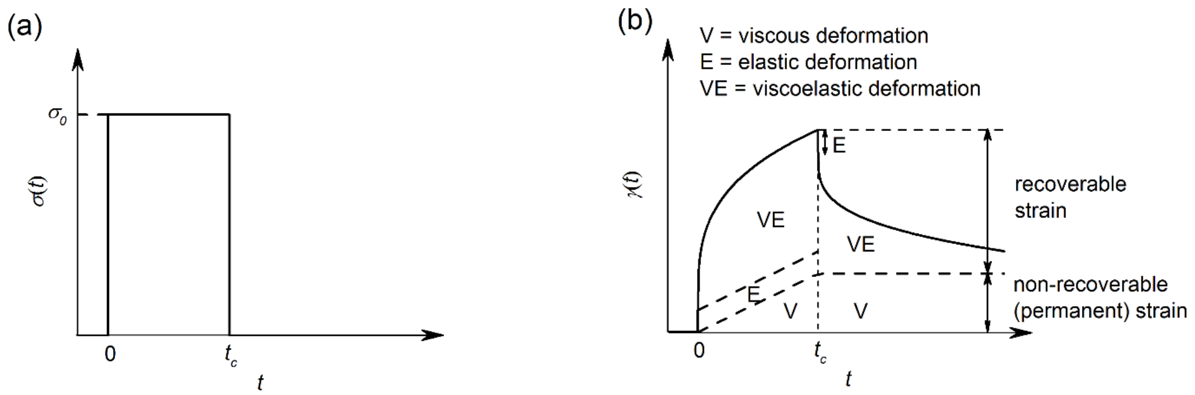

Fig. 1 Schematic of **a** the prescribed shear stress profile and **b** the resulting shear strain response in a creep-recovery experiment

The creep compliance can be divided into recoverable (elastic and viscoelastic) J_r and non-recoverable (viscous) J_{nr} components, respectively

$$J(t) = J_r(t) + J_{nr}(t) \qquad (3)$$

with

$$J_r(t) = J_0 + \psi(t) \qquad (4)$$

and

$$J_{nr}(t) = \frac{t}{\eta_0} \qquad (5).$$

J_0 is the instantaneous elastic compliance, ψ is the viscoelastic component of the creep compliance, and η_0 is the zero-shear viscosity.

In the range of linear viscoelasticity, the effect of combined load is equal to the sum of the effects of the individual loads (Lakes 1998), which is a consequence of the Boltzmann superposition principle superposition (BSP)

(Boltzmann 1874). Based on this principle, constitutive relations can be obtained that describe the material response to arbitrary load histories. The Boltzmann integral for the strain

$$\gamma(t) = \int_{-\infty}^{t} J(t-\xi)\frac{d\sigma(\xi)}{d\xi}d\xi \qquad (6)$$

represents the isothermal creep response of a linear viscoelastic material subjected to an arbitrary stress history $\sigma(\xi)$, where ξ is the time integration variable. In terms of the creep-recovery analysis, one of the most important consequences of the BSP is described by Meissner (1992) and referred to here as the "mirror rule". According to this rule, the stress removal is equivalent to applying a negative stress of equal magnitude σ_0 whilst preserving the original applied stress (see Fig. 2(a)). As stated by the BSP, the actual stress input is then the linear sum of these two stresses. In this case, the sum of the stresses is zero (as required by the definition of recovery in creep-recovery testing) because the positive and negative stress are equal in magnitude. Similarly, according to the BSP - and as shown in Fig. 2(b) - the strain response during the recovery period can be imagined to be a linear sum of two individual strain responses: the one induced by the positive creep stress (applied at time $t = 0$ in Fig. 2(a)) and the one induced by the negative creep stress (applied at time $t = t_c$ in Fig. 2(a)). Note that in this case these two imaginary strain responses are mirror images of each other, i.e. they have both identical magnitude and (shifted) time scales.

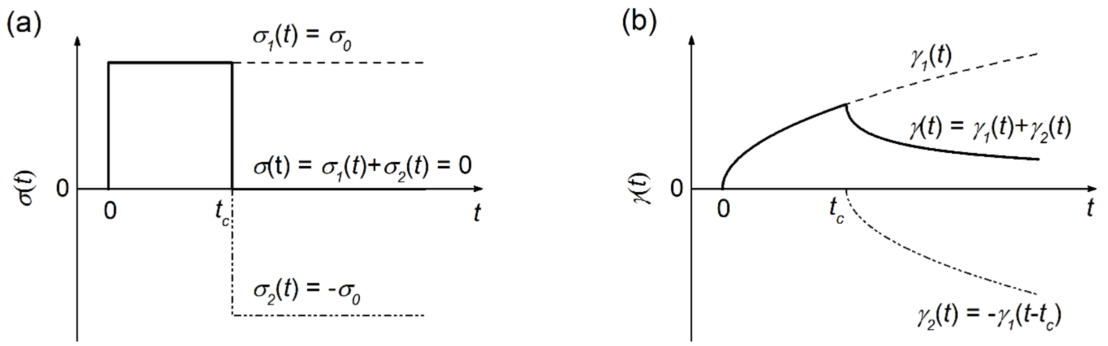

Fig. 2 Application of the Boltzmann superposition principle in the analysis of creep-recovery behavior: breakdown of the **a** stress input and **b** strain response during the recovery period according to the "mirror rule"

According to the theory of linear viscoelasticity, there is a relation between the SAOS and creep-recovery behavior of viscoelastic materials. This interrelationship can be conveniently expressed by using a discrete retardation time spectrum to describe the time-dependent strain response in creep and recovery (Eqs. (7) and (8), respectively) (Winter 1997; Ferry 1980; Macosko 1994).

$$\gamma(t) = \sigma_0 J(t) = \sigma_0\left[J_0 + \psi(t) + \frac{t}{\eta_0}\right] = \sigma_0\left[J_0 + \sum_{i=1}^{N-1} j_i\left(1 - e^{-\frac{t}{\lambda_i}}\right) + \frac{t}{\eta_0}\right] \quad \text{for } 0<t<t_c \qquad (7)$$

$$\gamma(t) = \sigma_0 J(t_r, t_c) = \sigma_0[J(t) - J(t_r)] = \sigma_0\left[\left(J_0 + \psi(t) + \frac{t}{\eta_0}\right) - \left(J_0 + \psi(t_r) + \frac{t_r}{\eta_0}\right)\right] = \sigma_0\left[\sum_{i=1}^{N-1} j_i\left(e^{-\frac{t_r}{\lambda_i}} - e^{-\frac{t}{\lambda_i}}\right) + \frac{t_c}{\eta_0}\right]$$
$$\text{for } t_c<t \qquad (8)$$

where j_i are the retardation strengths, λ_i are the retardation times, N is the number of relaxation modes, and the recovery time is defined as $t_r = t - t_c$. Note that these equations also satisfy the "mirror rule" as shown in Fig. 2.

Experiments on various glassy materials show that the elastic part of the creep compliance, J_0, is typically on the order of 10^{-9} Pa^{-1} (Donth 2001), and therefore it is often negligibly small compared with the viscoelastic and viscous components of the creep compliance. Consequently, the instantaneous elastic contribution to the creep compliance can well be neglected in the calculation of creep strain (Eq. 7).

The retardation time spectrum of the material determines the viscoelastic part of the creep compliance, $\psi(t)$. Methods of calculating the retardation time spectrum from the corresponding relaxation time spectrum are well known and based on the Laplace transform method (Baumgaertel and Winter 1989; Ferry 1980; Gross 1953; Leaderman 1958; Mead 1994). Because of this, the discrete retardation time spectrum, i.e. the values of retardation strengths j_i and retardation times λ_i, is most conveniently obtained by first calculating the discrete relaxation time spectrum from SAOS data (Baumgaertel and Winter 1989) using the following equations for the storage modulus G' and the loss modulus G'', respectively:

$$G'(\omega) = G_e + \sum_{i=1}^{N} g_i \frac{(\omega\tau_i)^2}{1+(\omega\tau_i)^2} \tag{9}$$

$$G''(\omega) = \sum_{i=1}^{N} g_i \frac{\omega\tau_i}{1+(\omega\tau_i)^2} \tag{10}$$

G_e is the equilibrium modulus (= 0 for viscoelastic liquids like bitumen), and g_i and τ_i are relaxation strengths and times, respectively. Notably, Eqs. (9) and (10) are mathematical representations of the dynamic moduli according to the generalized Maxwell model (GMM).

The material property influencing the viscous component of the creep compliance, t/η_0, is the zero-shear viscosity. Its value can be determined from the relaxation time spectrum, as shown by the following equation:

$$\eta_0 = \sum_{i=1}^{N} g_i \tau_i \tag{11}$$

3 Sequence of repeated creep recovery (RCR) experiments

The tools for modeling the strain response in a single creep-recovery experiment can be generalized to model the strain in a sequence of creep-recovery loadings. Within the linear viscoelastic range, such RCR experiment can be modeled as the linear superposition of many independent single creep-recovery tests, Eqs. (12) and (13). This idea of the linear superposition of strains in a RCR experiment is illustrated in Fig. 3 where both the strain contributions of single creep-recovery tests and the actual (total) RCR response are shown. Separate equations describe the strain during the Mth creep period

$$\gamma(t) = \sigma_0\left[\sum_{i=0}^{M-1} J(t-t_i) - \sum_{i=0}^{M-2} J(t-(t_i+t_c))\right] \qquad \text{for } t_i<t<(t_i+t_c) \tag{12}$$

and during the Mth recovery period

$$\gamma(t) = \sigma_0 \sum_{i=0}^{M-1}\left[J(t-t_i) - J(t-(t_i+t_c))\right] \qquad \text{for } (t_i+t_c)<t<t_{i+1} \tag{13}$$

where $t_i = i(t_c+t_r)$ is the duration of the sequence of i creep-recovery cycles. In the case of a single creep test ($M = 1$), the summation in the second term of Eq. (12) has the form $\sum_{i=0}^{-1} \ldots$ and is defined to be equal to zero.

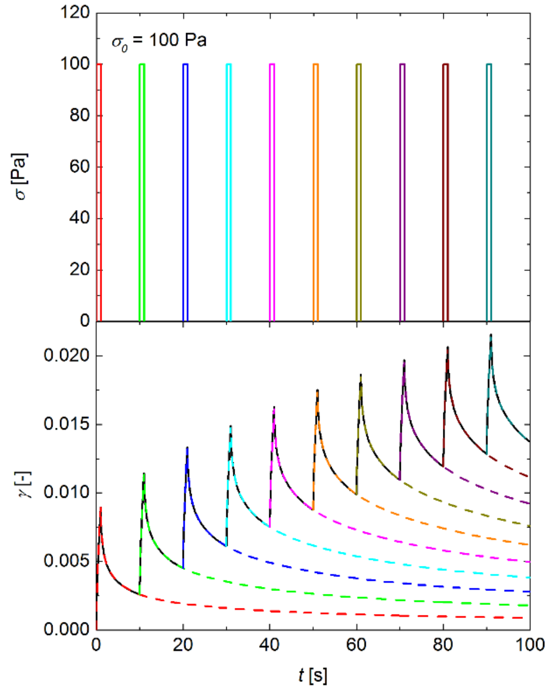

Fig. 3 Superposition of single creep-recovery tests to predict the strain response under RCR loading. The solid curve is the total accumulated strain and dashed curves represent the strain contributions from single creep-recovery tests

It should be noted that, as can be seen from Fig. 3, the strain may still be recovering at the end of each recovery period, i.e. the recovery is incomplete at the starting of the next creep-recovery cycle. This is particularly true for materials with significantly delayed elasticity and/or if the recovery periods are kept short in comparison to the characteristic material times. In this way, the remaining recoverable strain in one cycle will continue to contribute to the strain response during subsequent creep-recovery cycles, thereby increasing the overall amount of strain recovery. Wasage et al. (2007; 2010) already reported such evolution in the RCR response of a polymer-modified bitumen and attributed it to shear-induced structural changes in the material. Here we suggest that this explanation might not be correct. It is more likely that the apparent increase in strain recovery under RCR loading is due to delayed elasticity effects as described above. Experimental data and model predictions on the evolution of creep-recovery response are presented in Section "Comparison of predicted RCR response with measured data".

4 Materials and Methods

Various unmodified and modified bituminous binders were collected for this study to assess the performance of the presented model. Table 1 lists the investigated binders and their empirical properties (penetration, Ring-and-Ball softening point and penetration index). The elastomer is a commercial additive, which is widely used in bitumen modification, and the wax additive is a synthetic, commercially available Fischer-Tropsch wax.

Table 1 Overview of the investigated binders and their empirical properties. The type of bitumen modification is indicated in the sample code (B = no modification, E = elastomer modification, EW = elastomer+wax modification)

Sample code	Modification		Pen [1/10 mm]	$T_{R\&B}$ [°C]	PI [-]
	Additive	Level of modification			
B1	none	-	18	61.3	-0.83
B2	none	-	64	47.4	-1.31
B3	none	-	81	44.9	-1.44
E4	elastomer	Moderate	42	57.7	0.14
E5	elastomer	Moderate	60	61.5	1.80
E6	elastomer	High	75	65.4	3.20
EW7	elastomer + wax	High	31	92.9	4.71

Pen = penetration measured at 25 °C according to EN 1426 (2007a)

$T_{R\&B}$ = Ring-and-Ball softening point according to EN 1427 (2007b)

PI = penetration index = (1952-500×log(Pen)-20×$T_{R\&B}$)/(50×log(Pen)-$T_{R\&B}$-120)

Rheological measurements were performed with a stress-controlled Paar Physica MCR 500 rheometer. A Peltier plate and active hood controlled the test temperature with the accuracy of better than ±0.1 K avoiding temperature gradients within the test specimen. Isothermal frequency sweep measurements between 0.0628 to 62.8 rad/s were conducted in the temperature range of 10-70 °C at 10 K increments. A parallel plate geometry with a diameter of 25 mm and a gap of 1 mm was used in the temperature range of 40-70 °C, while a smaller plate diameter of 8 mm and a larger gap of 2 mm were used at the lower temperature range of 10-30 °C to minimize instrument compliance related errors (Liu et al. 2011; Schröter et al. 2006; Laukkanen 2017). RCR experiments were performed at 50 °C using a 25-mm parallel plate geometry with a 1-mm gap. The applied creep stress was varied from 100 to 6400 Pa, but only the RCR data measured at the lowest creep stress level of 100 Pa were analyzed to ensure the LVE response of the test materials (excluding the analysis presented in Section "Application to the assessment of the rutting resistance of bituminous binders"). The linear viscoelastic response of the investigated materials at 100 Pa creep stress was confirmed by plotting various rheological material parameters as a function of creep stress; selected results of this analysis have been published by Laukkanen et al. (2015). A sequence of a 1-second creep period followed by a 9-second recovery period was repeated ten times consecutively at each creep stress level. A careful analysis of the raw strain versus time data confirmed that the instrument-related artifacts described by Gabriel and Kaschta (1998) and Münstedt (2014) did not significantly influence our test results.

A well-defined specimen preparation protocol was followed throughout the study to ensure the consistency of the test results. A careful specimen preparation is essential in the rheological characterization of polymer and wax modified bituminous binders as differences in their thermal and loading histories may drastically change their rheological behavior (Soenen et al. 2006; Soenen et al. 2008; Soenen et al. 2005; Laukkanen and Soenen 2015). To prepare specimens for rheological testing, hot binder was poured in a silicon mold after the bulk binder sample had been carefully homogenized by manual stirring. The binder specimen was transferred from the mold to the rheometer, the gap of the rheometer was decreased to the trimming position (1.05 × the final measurement gap), and the test specimen was trimmed flush with the edges of the plate geometry using a hot spatula. After this, the gap was further decreased to the final measurement gap, and the temperature of the test specimen was let to equilibrate for 15 minutes prior to the start of the measurement.

Commercial Interactive Rheology Information Systems (IRIS) software (Winter and Mours 2006) was used in the analysis and plotting of rheological data.

5 Results and Discussion

5.1 Check for thermorheological simplicity

In order to have a complete description of the LVE properties of a material, it is desirable to construct the relaxation and retardation time spectra, used to calculate the RCR response as described in Section "Framework for predicting RCR response from SAOS data", from dynamic data that extends over a wide range of frequencies. Therefore, an effort is made to widen the frequency window of the experimental SAOS data by performing horizontal shifting according to the time-temperature superposition (TTS) principle. However, it should be remembered that the TTS principle is applicable only to thermorheologically simple materials. According to Dealy and Plazek (2009), the thermorheological simplicity of a material can be tested most conveniently by using linear scales in constructed master curve plots (Wood-Adams and Costeux 2001), by studying the smoothness of the loss tangent master curve (Winter 2013), or by plotting dynamic data in the Booij-Palmen (BP) plot of loss angle versus log$|G^*|$ (Booij and Palmen 1992). In the case of bituminous binders, it has been observed that the TTS principle does not hold for bitumens that contain high amounts of crystallizable fractions (waxes) or asphaltenes (Lesueur et al. 1996; Qin et al. 2014) and/or low amounts of resins (Loeber et al. 1998). Also, some polymer modified bituminous binders have been shown to exhibit thermorheologically complex behavior, especially when the amount of polymer is relatively high (Airey 2002; Pérez-Lepe et al. 2005).

To test the thermorheological simplicity of the investigated binders, and thus the applicability of the TTS principle, the BP plots were constructed and are shown in Fig. 4. The viscoelastic data of unmodified binders collapse into smooth monotonic BP curves and, thus, these binders can be viewed as thermorheologically simple. In the case of the elastomer modified binders, BP plots have more complex shape but are still relatively continuous. Therefore, also these binders can be judged to be thermorheologically rather simple. Finally, the binder modified both with elastomer and wax is as well observed to form a relatively smooth and continuous curve in the BP plot, and thus this binder too is thermorheologically nearly simple. As a side note, it can be mentioned that binders B1, B2, B3, E4 and E5 can be considered to be viscoelastic liquids as evidenced by the fact that phase angle values asymptotically approach the value of 90° at low G^* values. On the contrary, the phase angle values of binders E6 and EW7 appear to diverge from 90° at low G^* values, indicating the semi-solid nature of these materials. In this case, the semi-solid characteristics are most likely due to the formation of a continuous elastomeric network within the binder that is modified with a high amount of polymer (Airey 2003).

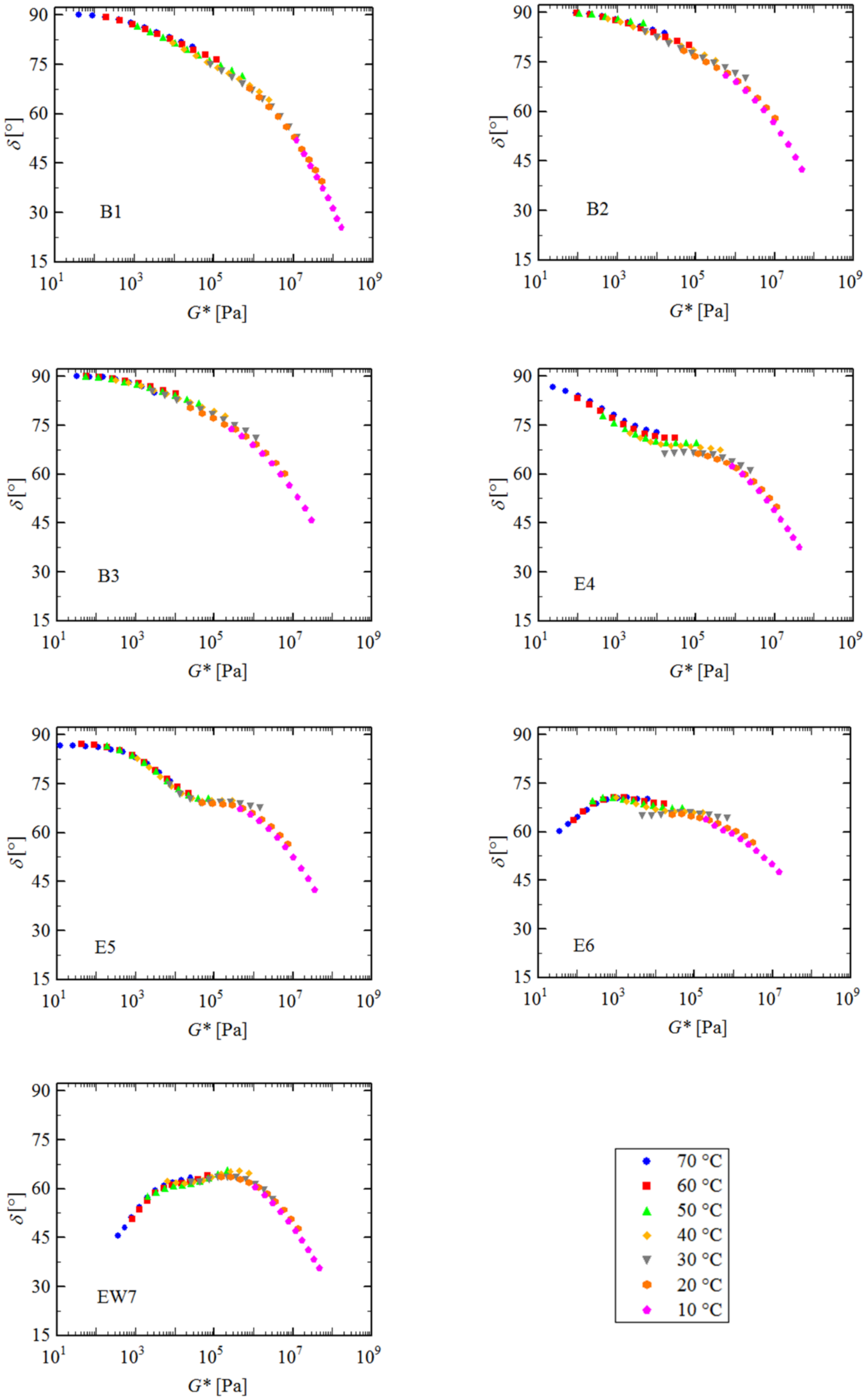

Fig. 4 Booij-Palmen plots of the investigated binders

5.2 Construction of master curves and spectra calculation

Although it was observed that not all the investigated binders are perfectly thermorheologically simple, an effort was made to construct master curves for these binders. Master curves of dynamic material functions (storage modulus, G'; loss modulus, G''; and loss tangent, tan δ) were obtained by using the horizontal (frequency) shifting routine of the IRIS software (Winter and Mours 2006), and are shown in Fig. 5 with the fits of the GMM at the reference temperature of 50 °C. The horizontal shift factors a_T obtained from the construction of the master curves are found to follow a Williams-Landel-Ferry (WLF) type of temperature dependence (Williams et al. 1955) (not shown here for brevity).

The loss tangent master curves in Fig. 5 do not show noticeable discontinuities, therefore indicating at least a moderate applicability of the TTS principle for all the investigated binders. At the low-frequency regime, the storage and loss modulus master curves of the unmodified binders are characterized by the slopes of 2 and 1, respectively, indicating Newtonian flow behavior in the terminal zone. In contrast, the values of the low-frequency slopes are generally smaller for the modified binders demonstrating the non-Newtonian nature of these binders at low frequencies or high temperatures. Furthermore, the storage modulus master curves of binders E6 and EW7 appear to plateau at low frequencies, reinforcing the observation of the semi-solid nature of these binders (cf. Section "Check for thermorheological simplicity").

Relaxation time spectra of the binders were calculated by fitting Eqs. (9) and (10) to the time-temperature shifted dynamic data using the method of Baumgaertel and Winter (1989). Upon the calculation of the relaxation time spectrum, the values of relaxation strength g_i and time τ_i of each individual relaxation mode are obtained. Further, the values of retardation strengths j_i and times λ_i are acquired, defining the discrete retardation time spectra of the binders. The values of the relaxation and retardation parameters for the investigated binders are listed in the Electronic Supplementary Material for this article, with the values of mode density, N/decade, zero-shear viscosity, η_0, and instantaneous creep compliance, J_0.

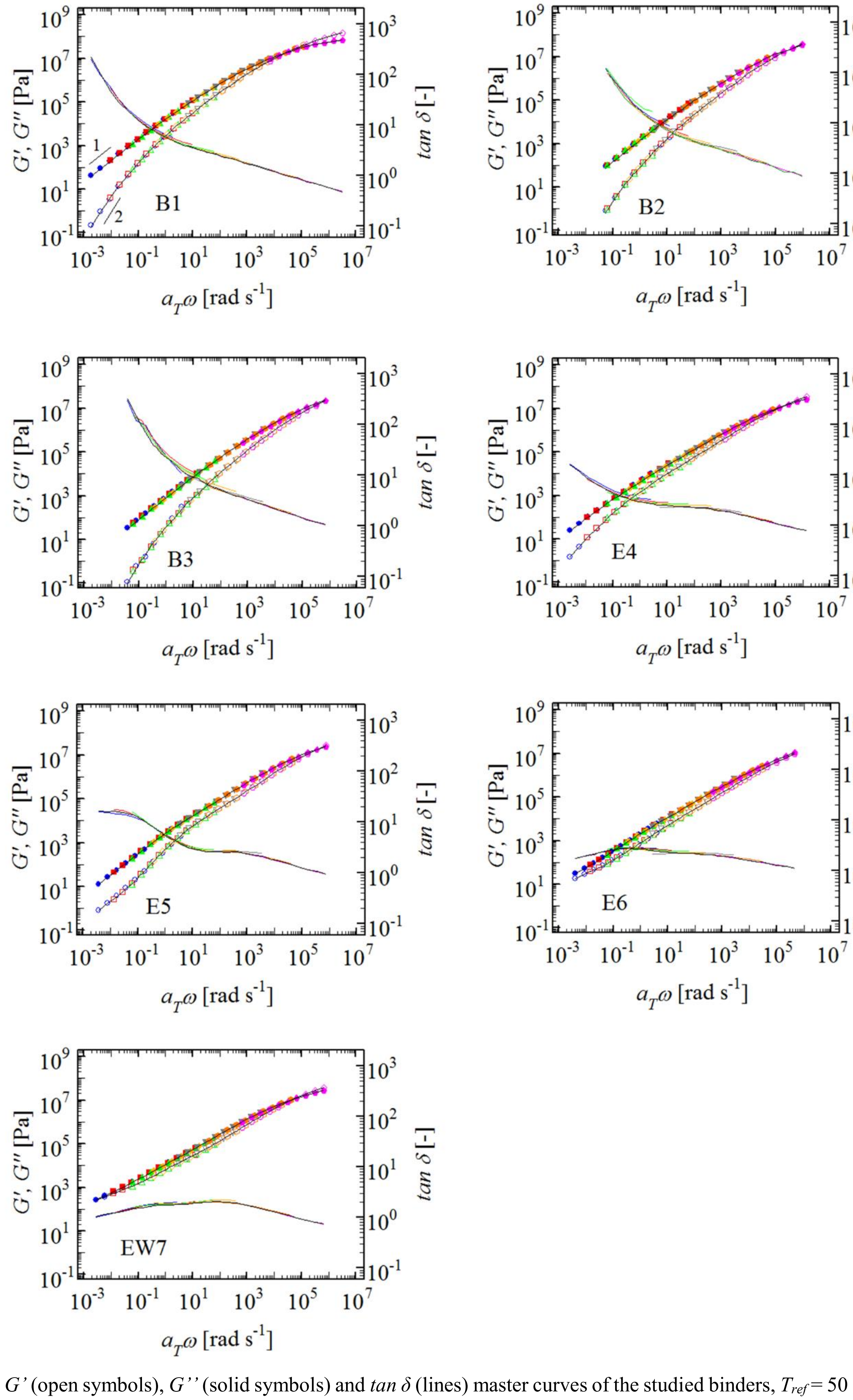

Fig. 5 *G'* (open symbols), *G''* (solid symbols) and *tan δ* (lines) master curves of the studied binders, T_{ref} = 50 °C. Different colors indicate different measurement temperatures as in Fig. 4. Fits of the GMM are shown as black lines

5.3 Comparison of predicted RCR response with measured data

In order to assess the validity of the used model, the predicted RCR strain is compared with experimental (measured) RCR data. As shown in Fig. 6, experimental data compare well with predictions for the unmodified binders. However, in the case of modified binders, strain accumulation is slightly but systematically overestimated, the relative error of the model predictions being ≤20 %. These minor deviations between the predicted and measured RCR response can be attributed to the lack of experimental information of the binders' long relaxation time modes as described later in this section. Indeed, the predicted RCR response deviates most from the measured one in highly modified binders E6 and EW7 that presumably exhibit very long relaxation modes (much longer than those listed in the Electronic Supplementary Material for this article) and, consequently, semi-solid like characteristics at low frequencies or high temperatures (Figs. 4 and 5). However, we want to underline that, in general, the observed model deviations can still be regarded as relatively small, especially when considering that they are within the repeatability limits of this test method (a detailed analysis of the repeatability of the RCR test results has been published elsewhere (Soenen et al. 2013)). Moreover, the reported inaccuracies in the model predictions are typically insignificantly small compared to the large differences between the RCR responses of different binders (the bottom right part of Fig. 6). With the consideration of the aforementioned factors, the accuracy of our model predictions can be deemed acceptable both in the case of unmodified and modified bituminous binders.

To further assess the accuracy of the presented model, some parameters for describing RCR response were defined and their measured and predicted values were compared. Firstly, the measured and predicted values of the average strain generated during the 1-second creep periods were calculated and compared, see Fig. 7(a). In this figure the data points corresponding to each of the binders lie on the line of equality, thus evidencing a good agreement between the measured and predicted values of the parameter. Similarly, the predicted and measured values of the average strain recovery during the 9-second recovery periods (expressed as a percentage of the preceding creep strain) were calculated and are plotted against each other in Fig. 7(b). Also in this case a good correspondence between the measured and predicted values is observed. Lastly, Fig. 7(c) compares the predicted and measured values of the accumulated strain at the end of the RCR experiment, and yet again a very good agreement is found. We also note that our modeling approach is able to rank the investigated binders in the correct relative order in each of Figs. 7(a)-(c). Conclusively, the analysis described above demonstrates the general ability of the presented methodology to predict strain development both in creep and in recovery under RCR loading.

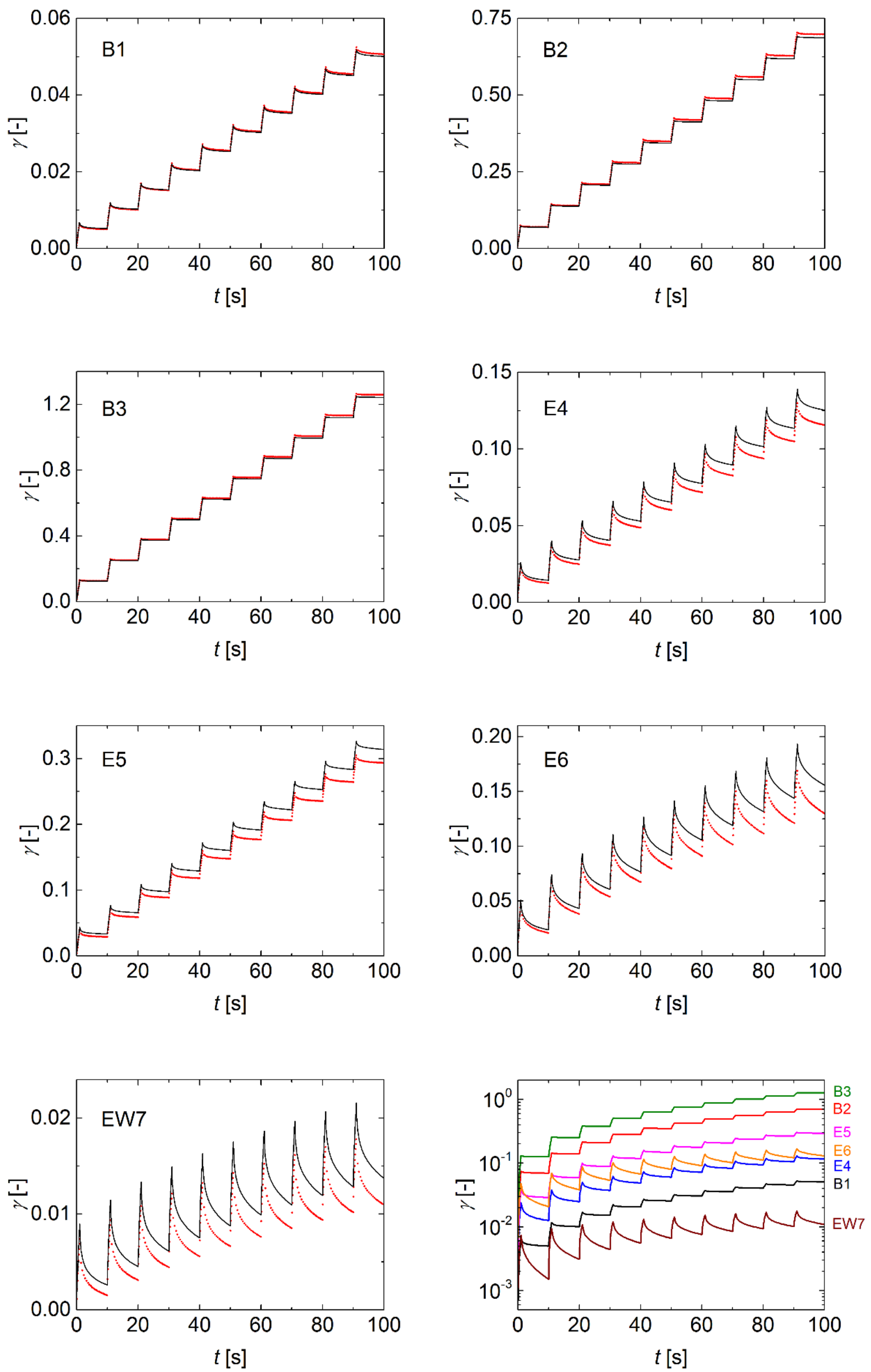

Fig. 6 Comparison of predicted (solid black curve) and measured (filled red circles) strain responses under RCR loading (note different scaling on the y-axes). The last of the plots compares the measured RCR strain of different binders (note that the y-axis is plotted on a logarithmic scale to accommodate the broad strain range)

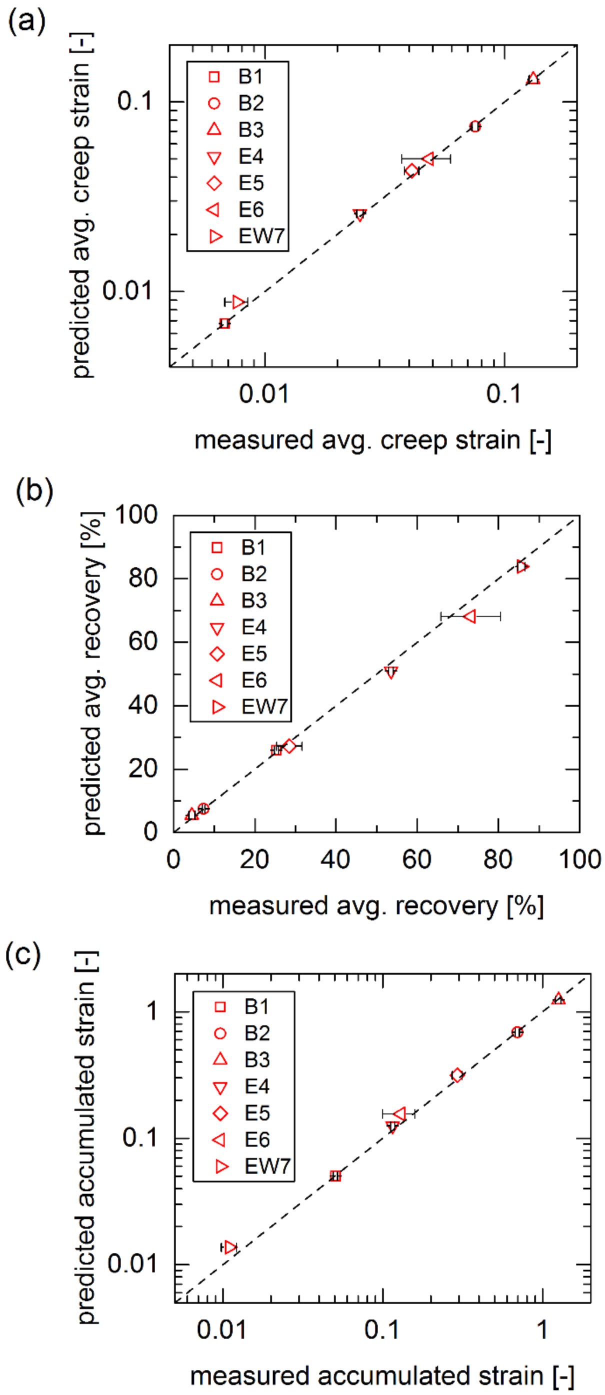

Fig. 7 Plots of predicted versus measured values of **a** average creep strain, **b** average percent recovery and **c** accumulated strain at the end of the RCR experiment. The lines of equality are shown, and the error bars correspond to the repeatability standard deviations determined by Soenen et al. (2013)

However, it is not always sufficient to investigate only the average values of creep and recovery properties as the strain response of a material may evolve remarkably under RCR loading (Laukkanen et al. 2015). From among the investigated materials, evolution in the strain response was observed in highly modified binders E6 and EW7. In these binders the amount of recovery increases in successive creep-recovery cycles, leading to the decrease in the rate of strain accumulation (see Fig. 3 as an example). This type of evolution in the material response can be attributed to the incomplete recovery that is caused by the existence of long-term elasticity. In other words, in highly modified binders that exhibit long-term relaxation modes not all the recovery occurs during the 9-second recovery period immediately following the creep loading, but recovery persists also during the following creep-recovery cycles. The ability of the presented model to predict this evolution in the strain response is illustrated in Fig. 8 where the measured and predicted evolution in the strain response of binder E6 are shown and compared. It is observed that, indeed, the relative amount of recovery increases significantly under RCR loading, from ~57 % in the first creep-recovery cycle to ~82 % in the tenth creep-recovery cycle), and the model predictions are found to follow this trend satisfactorily. The slight systematic underestimation of the amount of recovery can be explained by the lack of experimental information on the long relaxation time modes of the binder, as discussed more fully later in this paper. Similarly, adequate predictions of the evolution of strain response in binder EW7 were obtained by using the presented methodology (the figure is not shown here for brevity).

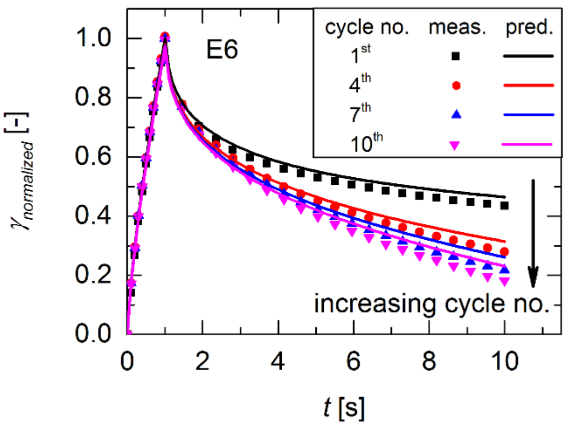

Fig. 8 Measured and predicted evolution in the strain response of binder E6 under RCR loading. The curves are normalized with respect to the strain at the end of the creep period

It is widely known that a successful conversion between creep and dynamic viscoelastic functions requires the timescales to be matched (Emri et al. 2005; Ferry 1980; Katicha et al. 2008). In RCR experiments the relevant (effective) timescales are defined by the total durations of loading and unloading periods (Soenen et al. 2006); in our case the total loading time is 10 × 1 = 10 seconds and the total unloading time is 10 × 9 = 90 seconds. Therefore, the strain response towards the end of our RCR experiment corresponds to relatively long loading times. In our modeling approach, we measure high-temperature SAOS data and utilize the time-temperature superposition principle to extend the experimental data window to lower frequencies (or to longer loading times, equivalently). The importance of this time-temperature shifting procedure in the prediction of RCR response is investigated further in Fig. 9. This figure shows the original predictions of the RCR response together with the predictions that have been generated without utilizing time-temperature shifting (i.e. by using only the frequency sweep data measured at 50 °C). These predictions are shown only for highly modified binders E6 and EW7 that exhibit significant long-term elasticity. As expected, the predictions start to deviate from each other towards the end of the test, so that the prediction generated from the time-temperature shifted data is in a better agreement with the experimental RCR data than the prediction calculated solely based on the frequency sweep data measured at 50 °C. However, as noted already earlier, even the prediction calculated from the time-temperature shifted data is not perfect but overestimates the amount of strain accumulation. Therefore, it is clear that SAOS data would need to be measured at even higher temperatures (above 70 °C) in order to properly capture the long-term elasticity and to further improve the accuracy of the RCR predictions.

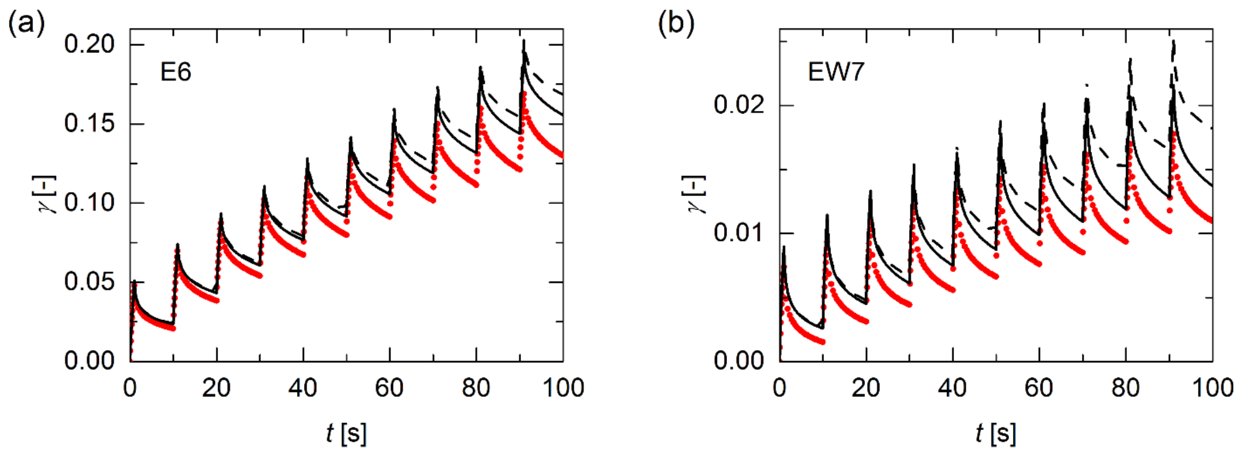

Fig. 9 Comparison of the RCR response predicted from time-temperature shifted SAOS data (solid black curve) and from isothermal SAOS data measured at 50 °C (dashed black curve). Filled red circles represent measured data. Plots are shown only for highly modified binders **a** E6 and **b** EW7 that possess significant long-term elasticity

Furthermore, we emphasize that the use of high-temperature SAOS data in the prediction of RCR behavior becomes ever more important when the total loading and unloading times are increased. This is demonstrated in Fig. 10 which shows strain response for moderately modified binder E4 (showing liquid-like terminal behavior, see Figs. 4 and 5) during 520-second creep and recovery periods. This figure also depicts two predictions of the strain response calculated in the same way as in Fig. 9. The two model predictions are observed to follow the experimental strain data very accurately during the first 100 seconds of creep (magnified in the inset figure). However, at longer loading times and during recovery the prediction calculated solely based on the frequency sweep data measured at 50 °C deviates clearly from the measured data. On the other hand, fairly good predictions of the long-term creep and recovery behavior can be obtained when time-temperature shifted SAOS data, including high-temperature data, is utilized in the model calculations. It can therefore be concluded that even when the material of interest does not exhibit significant long-term elasticity, it is important to utilize high-temperature SAOS data and time-temperature shifting in the prediction of (repeated) creep-recovery behavior when the (total) loading and unloading times are long.

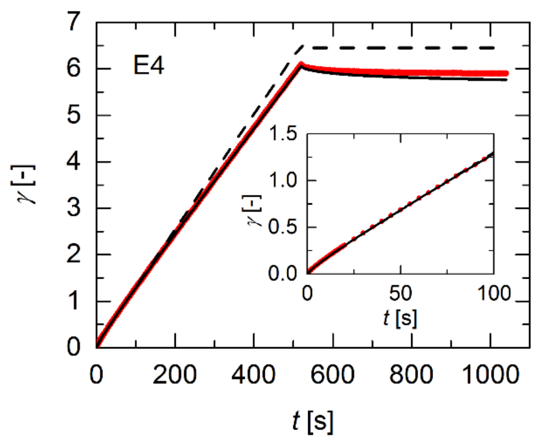

Fig. 10 Comparison of the long-term creep-recovery response of binder E4 predicted from time-temperature shifted SAOS data (solid curve) and from isothermal SAOS data measured at 50 °C (dashed curve). Filled circles represent measured data. The inset figure shows a magnification of the first 100 s of the creep phase

5.4 Application to the assessment of the rutting resistance of bituminous binders

As indicated in the bottom right part of Fig. 6, RCR is a sensitive indicator between small differences in materials. The asphalt industry routinely relies on RCR experiments to select bituminous binders for performance at high service temperatures. A test protocol called 'Multiple Stress Creep Recovery (MSCR) test' is widely used, especially in the United States, to grade binders according to their resistance against permanent deformation (D'Angelo et al. 2007). This test method consists of ten consecutive creep-recovery cycles at 100 Pa creep stress followed by another ten creep-recovery cycles at 3200 Pa creep stress. Each creep-recovery cycle is comprised of 1-second creep phase and 9-second recovery phase. From the collected strain versus time data, the average values of non-recoverable creep compliance, J_{nr}, and percent recovery, *%R*, are calculated at both 100 and 3200 Pa creep stress levels.

$$J_{nr} = \frac{\sum_{i=1}^{M} \frac{\gamma_{10,i}}{\sigma_0}}{M} \tag{14}$$

$$\%R = \frac{\sum_{i=1}^{M} \frac{\gamma_{1,i}-\gamma_{10,i}}{\gamma_{1,i}}}{M} \times 100 \tag{15}$$

where $M = 10$ is the number of creep-recovery cycles at each creep stress level, $\gamma_{10,i}$ is the strain value at the end of the recovery portion of the *i*th creep-recovery cycle, and $\gamma_{1,i}$ is the strain value at the end of the creep portion of the *i*th creep-recovery cycle. The permanent deformation in a binder under RCR loading, J_{nr}, has been shown to correlate linearly with the rut depth in asphalt mixtures and pavements (D'Angelo 2009; Laukkanen et al. 2015; Zhang et al. 2015). Correspondingly, *%R* relates to the elastic response of polymer modifier in a binder, which helps to discriminate between the dump-and-stir types of polymer modified binders and those that have been optimally dispersed (D'Angelo and Dongré 2009). A comparison of the test parameters, $J_{nr,diff}$ and $\%R_{diff}$, at creep stresses 100 Pa and 3200 Pa,

$$J_{nr,diff} = \frac{J_{nr,3200}-J_{nr,100}}{J_{nr,100}} \times 100 \tag{16}$$

$$\%R_{diff} = \frac{R\%_{100}-R\%_{3200}}{R\%_{100}} \times 100 \tag{17}$$

assess the stress sensitivity of binders. A more comprehensive description of the test protocol and related data analysis are presented in AASHTO T350 (2014a) and ASTM D7405 (2015) standards.

From the viewpoint of an asphalt engineer, it is interesting to study whether the presented methodology could be used to predict the values of J_{nr} and *%R* parameters from SAOS data. Most importantly, one would like to know if it is possible to estimate the value of J_{nr} parameter at 3200 Pa creep stress level; this parameter is known to well describe the binder contribution to asphalt mixture permanent deformation (D'Angelo 2009). It has been reported earlier that while the unmodified binders investigated in this study exhibit only moderate nonlinearity under these testing conditions (T = 50 °C, σ_0 = 3200 Pa), some of the modified binders are highly stress-sensitive and show highly nonlinear properties (Laukkanen et al. 2015; Soenen et al. 2013). Therefore, we must acknowledge that using our linear viscoelastic modeling approach to predict RCR response at 3200 Pa creep stress is not theoretically sound. However, our aim here is only to test whether approximate estimates of the J_{nr} and *%R* parameters at 3200 Pa creep stress can be obtained empirically in a very simple and practical manner.

Figure 11 plots the LVE predictions of J_{nr} and *%R* against the measured values of these parameter at 3200 Pa creep stress. In this case, a very strong correlation can be found between the measured and predicted values of both of these parameters. Therefore, we suggest that, in most cases, the presented modeling approach can be used to calculate a first approximation of the RCR properties at the creep stress level of 3200 Pa. We note that the accuracy of these approximations would be significantly tolerated only in extremely stress-sensitive binders that are forbidden in road construction (AASHTO M332 standard (2014b) allows only binders with $J_{nr,diff}$ < 75 % to be used in paving applications).

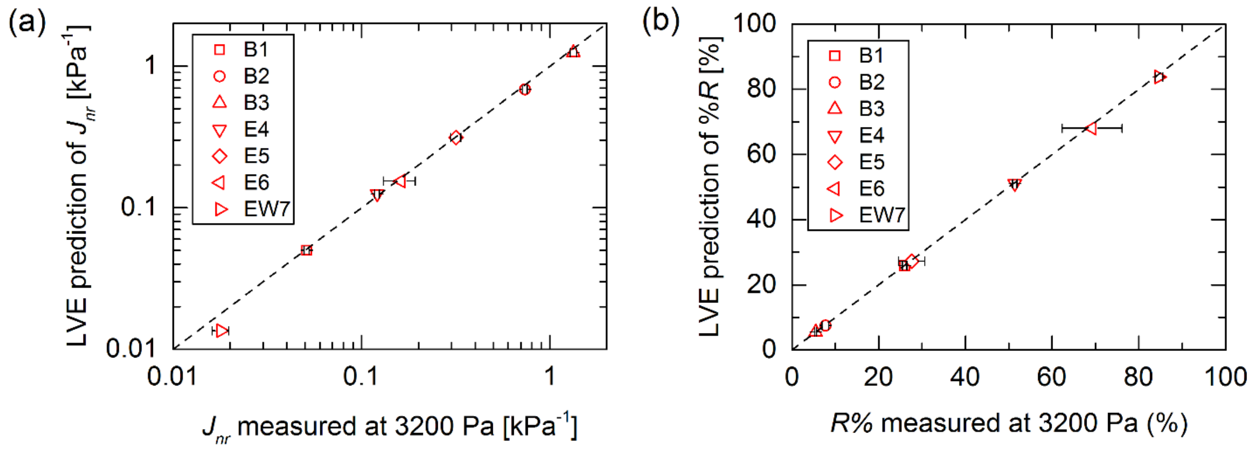

Fig. 11 Plots of the LVE predictions versus measured values of the **a** J_{nr} and **b** *%R* parameters at 3200 Pa creep stress. Solid lines represent lines of equality and error bars correspond to the repeatability standard deviations determined by Soenen et al. (2013)

Figure 12 shows another way to evaluate the feasibility of using the LVE prediction of J_{nr} as the first approximation of binder rutting resistance. Here the LVE predictions of the binders' J_{nr} values are plotted against the rutting performance of the corresponding asphalt mixtures, as measured by the power-law exponent *b* derived from the wheel tracking test (WTT) results (see Laukkanen et al. (2015) for details). Note that in these WTT tests, the asphalt mixtures differed only by the type of bituminous binder used, and therefore the value of the power-law exponent *b* can be directly related to the binder properties. The figure reveals a strong correlation ($R^2 = 0.975$) between the two variables that is, in fact, practically as strong as the correlation between the measured values of J_{nr} at 3200 Pa and the power-law exponent *b* (see Fig. 10 in Laukkanen et al. (2015)). This analysis further demonstrates the feasibility of using the LVE prediction of J_{nr} as a simple approximation of the rutting resistance of bituminous binders.

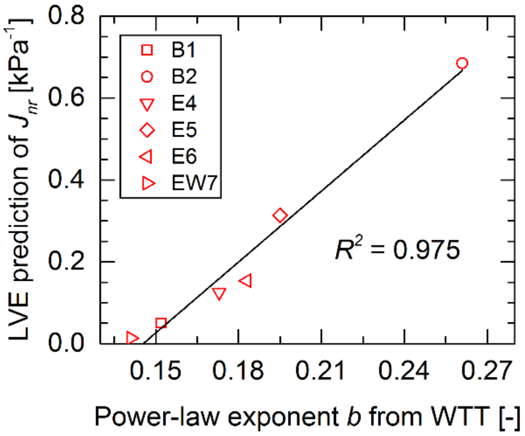

Fig. 12 Plot of the LVE prediction of J_{nr} versus the power-law exponent b derived from the asphalt mixture WTT results. Binder B3 is omitted from the analysis due to the experimental limitations of WTT (Laukkanen et al. 2015)

6 Conclusions

In this paper, we presented a framework for predicting strain accumulation under repeated creep-recovery (RCR) loading from small-amplitude oscillatory shear (SAOS) experiments, and applied this framework to the specific case of bituminous binders. Predictions of the shear strain response under RCR loading are obtained through the calculation of the relaxation and retardation time spectra and by utilizing a linear superposition of strain according to the Boltzmann superposition principle. It was found that the RCR response of unmodified binders can be accurately predicted using the presented methodology, but in modified binders the strain accumulation is slightly but systematically overestimated. This deviation in the model predictions is attributed to the lack of experimental information on the long relaxation time modes of the modified binders, leading to the underestimation of long-term elasticity. Consequently, low-frequency (high-temperature) SAOS data are needed to obtain accurate predictions of RCR behavior when material exhibits significant elasticity. It was also demonstrated that the evolution in the strain response under RCR loading, caused by incomplete recovery, can be successfully predicted using the presented modeling methodology.

As RCR measurements often suffer from experimental artifacts and poor repeatability and reproducibility, the presented modeling approach may be useful in obtaining an accurate description of the RCR behavior of different viscoelastic materials (given that extensive SAOS or other type of linear viscoelastic data are available). One of the potential application areas of this methodology is asphalt industry; analysis of our results showed that the predicted RCR properties can be used as a simple first approximation to estimate the rutting resistance of bituminous binders. However, the authors acknowledge that predictions of nonlinear viscoelastic RCR behavior would be needed to obtain more accurate predictions of binder rutting resistance, but this remains a subject for further study.

References

Airey, G.D.: Rheological properties of styrene butadiene styrene polymer modified road bitumens. Fuel 82, 1709-1719 (2003)

Airey, G.D.: Use of black diagrams to identify inconsistencies in rheological data. Road Mater Pavement 3, 403-424 (2002)

American Association of State Highway and Transportation Officials: AASHTO T350: Standard Method of Test for Multiple Stress Creep Recovery (MSCR) Test of Asphalt Binder Using a Dynamic Shear Rheometer (DSR). Washington, DC (2014a)

American Association of State Highway and Transportation Officials: AASHTO M332: Standard Specification for Performance-Graded Asphalt Binder Using Multiple Stress Creep Recovery (MSCR) Test. Washington, DC (2014b)

American Society for Testing and Materials: ASTM D7405: Standard Test Method for Multiple Stress Creep and Recovery (MSCR) of Asphalt Binder Using a Dynamic Shear Rheometer. West Conshohocken, PA (2015)

Bahia, H.U., Zhai, H., Zeng, M., Hu, Y., Turner, P.: Development Of Binder Specification Parameters Based On Characterization Of Damage Behavior. Assoc Asphalt Paving Technol 70, 442-470 (2001)

Baumgaertel, M., Winter, H.H.: Determination of discrete relaxation and retardation time spectra from dynamic mechanical data. Rheol Acta 28, 511-519 (1989)

Boltzmann, L.: Zur Theorie der Elastischen Nachwirkungen. Sitzungsber. Kaiserl. Akad. Wiss. Wien, Math. - Naturwiss. 70, 275-306 (1874)

Booij, H.C., Palmen, J.H.M.: Linear viscoelastic properties of melts of miscible blends of poly (methylmethacrylate) with poly (ethylene oxide). In: Moldenaers, P., Keunings, R. (eds.) Theoretical and applied rheology, pp. 321-323. Elsevier, Brussels (1992)

D'Angelo, J., Dongré, R.: Practical use of multiple stress creep and recovery test: characterization of styrene-butadiene-styrene dispersion and other additives in polymer-modified asphalt binders. Transp Res Rec 2126, 73-82 (2009)

D'Angelo, J., Kluttz, R., Dongre, R.N., Stephens, K., Zanzotto, L.: Revision of the Superpave High Temperature Binder Specification: The Multiple Stress Creep Recovery Test. J Assoc Asphalt Pavement 76, 123-162 (2007)

D'Angelo, J.A.: The relationship of the MSCR test to rutting. Road Mater Pavement 10, 61-80 (2009)

Dealy, J., Plazek, D.: Time-temperature superposition—a users guide. Rheol Bull 78, 16-31 (2009)

Delgadillo, R., Nam, K., Bahia, H.: Why do we need to change G*/sinδ and how?. Road Materials and Pavement Design 7, 7-27 (2006)

Donth, E.: The glass transition: relaxation dynamics in liquids and disordered materials. Springer, Berlin, Germany (2001)

Emri, I., von Bernstorff, B.S., Cvelbar, R., Nikonov, A.: Re-examination of the approximate methods for interconversion between frequency-and time-dependent material functions. J. Non Newtonian Fluid Mech. 129, 75-84 (2005)

European Committee for Standardization: EN 1426: Bitumen and bituminous binders. Determination of needle penetration. Brussels (2007a)

European Committee for Standardization: EN 1427: Bitumen and bituminous binders: Determination of the softening point, Ring and Ball method. Brussels (2007b)

Ferry, J.D.: Viscoelastic properties of polymers. John Wiley & Sons, New York (1980)

Gabriel, C., Kaschta, J.: Comparison of different shear rheometers with regard to creep and creep recovery measurements. Rheol Acta 37, 358-364 (1998)

Gross, B.: Mathematical structure of the theories of viscoelasticity. Hermann & Cie., Paris (1953)

Katicha, S., Flintsch, G.W., Loulizi, A., Wang, L.: Conversion of testing frequency to loading time applied to the Mechanistic-Empirical Pavement Design Guide. Transp Res Rec 2087, 99-108 (2008)

Lakes, R.S.: Viscoelastic solids. CRC press, Boca Raton, FL (1998)

Laukkanen, O.V.: Small-diameter parallel plate rheometry: a simple technique for measuring rheological properties of glass-forming liquids in shear. Rheol Acta 56, 661-671 (2017)

Laukkanen, O.V., Soenen, H.: Rheological characterization of wax modified bituminous binders: Effect of specimen preparation and thermal history. Constr Build Mater 95, 269-278 (2015)

Laukkanen, O.V., Soenen, H., Pellinen, T., Heyrman, S., Lemoine, G.: Creep-recovery behavior of bituminous binders and its relation to asphalt mixture rutting. Mater Struct 48, 4039-4053 (2015)

Leaderman, H.: Viscoelasticity phenomena in amorphous high polymeric systems. In: Eirich, F. (ed.) Rheology, Theory and Applications, pp. 1-61. Academic Press, New York (1958)

Lesueur, D., Gerard, J., Claudy, P., Letoffe, J., Planche, J., Martin, D.: A structure-related model to describe asphalt linear viscoelasticity. J. Rheol. 40, 813-836 (1996)

Liu, C., Yao, M., Garritano, R.G., Franck, A.J., Bailly, C.: Instrument compliance effects revisited: linear viscoelastic measurements. Rheol Acta 50, 537-546 (2011)

Loeber, L., Muller, G., Morel, J., Sutton, O.: Bitumen in colloid science: a chemical, structural and rheological approach. Fuel 77, 1443-1450 (1998)

Macosko, C.W.: Rheology: principles, measurements, and applications. Wiley-VCH, New York (1994)

Mead, D.: Numerical interconversion of linear viscoelastic material functions. J Rheol 38, 1769-1795 (1994)

Meissner, J.: Experimental problems and recent results in polymer melt rheometry. Makromol. Chem. , Macromol. Symp. 56, 25-42 (1992)

Mezger, T.G.: The rheology handbook: for users of rotational and oscillatory rheometers. Vincentz Network GmbH & Co KG, Hannover (2006)

Münstedt, H.: Rheological experiments at constant stress as efficient method to characterize polymeric materials. J. Rheol. 58, 565-587 (2014)

Pérez-Lepe, A., Martínez-Boza, F., Gallegos, C.: Influence of polymer concentration on the microstructure and rheological properties of high-density polyethylene (HDPE)-modified bitumen. Energy Fuels 19, 1148-1152 (2005)

Qin, Q., Farrar, M.J., Pauli, A.T., Adams, J.J.: Morphology, thermal analysis and rheology of Sasobit modified warm mix asphalt binders. Fuel 115, 416-425 (2014)

Schröter, K., Hutcheson, S., Shi, X., Mandanici, A., McKenna, G.: Dynamic shear modulus of glycerol: Corrections due to instrument compliance. J. Chem. Phys. 125, 214507 (2006)

Soenen, H., Lu, X., Redelius, P.: The morphology of bitumen-SBS blends by UV microscopy: An evaluation of preparation methods. Road Mater Pavement 9, 97-110 (2008)

Soenen, H., Blomberg, T., Pellinen, T., Laukkanen, O.V.: The multiple stress creep-recovery test: a detailed analysis of repeatability and reproducibility. Road Mater Pavement 14, 2-11 (2013)

Soenen, H., De Visscher, J., Vanelstraete, A., Redelius, P.: Influence of thermal history on rheological properties of various bitumen. Rheol Acta 45, 729-739 (2006)

Soenen, H., De Visscher, J., Vanelstraete, A., Redelius, P.: The influence of thermal history on binder rutting indicators. Road Mater Pavement 6, 217-238 (2005)

Wasage, T., Statsna, J., Zanzotto, L.: Repeated loading and unloading tests of asphalt binders and mixes. Road Materials and Pavement Design 11, 725-744 (2010)

Wasage, T., Cantu, M., Stastna, J., Polacco, G., Zanzotto, L.: Role of viscosity in dynamic creep tests in conventional, oxidized, and polymer-modified asphalts. Transp Res Rec 1998, 56-64 (2007)

Williams, M.L., Landel, R.F., Ferry, J.D.: The temperature dependence of relaxation mechanisms in amorphous polymers and other glass-forming liquids. J. Am. Chem. Soc. 77, 3701-3707 (1955)

Winter, H.H.: Glass transition as the rheological inverse of gelation. Macromolecules 46, 2425-2432 (2013)

Winter, H.H.: Analysis of dynamic mechanical data: inversion into a relaxation time spectrum and consistency check. J. Non Newtonian Fluid Mech. 68, 225-239 (1997)

Winter, H.H., Mours, M.: The cyber infrastructure initiative for rheology. Rheol Acta 45, 331-338 (2006)

Wood-Adams, P., Costeux, S.: Thermorheological behavior of polyethylene: effects of microstructure and long chain branching. Macromolecules 34, 6281-6290 (2001)

Zhang, J., Walubita, L.F., Faruk, A.N., Karki, P., Simate, G.S.: Use of the MSCR test to characterize the asphalt binder properties relative to HMA rutting performance–A laboratory study. Constr. Build. Mater. 94, 218-227 (2015)